

Available online at www.sciencedirect.com

ScienceDirect

www.elsevier.com/locate/jes

JES

JOURNAL OF
ENVIRONMENTAL
SCIENCESwww.jesc.ac.cn

Cause of PM_{2.5} pollution during the 2016-2017 heating season in Beijing, Tianjin, and Langfang, China

Nini Pang^{1,2}, Jian Gao^{2,*}, Fei Che², Tong Ma², Su Liu³, Yan Yang²,
Pusheng Zhao⁴, Jie Yuan⁵, Jiayuan Liu², Zhongjun Xu^{1,*}, Fahe Chai²

¹Department of Environmental Science and Engineering, Beijing University of Chemical Technology, Beijing 100029, China

²Chinese Research Academy of Environmental Sciences, Beijing 100012, China

³Qingdao Huasi Environmental Protection Technology Co., Ltd., Qingdao 266199, China

⁴Institute of Urban Meteorology, China Meteorological Administration, Beijing 100089, China

⁵Tianjin Environmental Monitoring Center, Tianjin 300191, China

ARTICLE INFO

Article history:

Received 24 September 2019

Revised 31 January 2020

Accepted 17 March 2020

Available online 7 May 2020

Keywords:

Heating season

Fine particulate matter

Chemical components

Formation mechanism

Regional pollution episodes

ABSTRACT

To investigate the cause of fine particulate matter (particles with an aerodynamic diameter less than 2.5 μm, PM_{2.5}) pollution in the heating season in the North China Plain (specifically Beijing, Tianjin, and Langfang), water-soluble ions and carbonaceous components in PM_{2.5} were simultaneously measured by online instruments with 1-hr resolution, from November 15, 2016 to March 15, 2017. The results showed extreme severity of PM_{2.5} pollution on a regional scale. Secondary inorganic ions (SNA, i.e., NO₃⁻+SO₄²⁻+NH₄⁺) dominated the water-soluble ions, accounting for 30%-40% of PM_{2.5}, while the total carbon (TC, i.e., OC + EC) contributed to 26.5%-30.1% of PM_{2.5} in the three cities. SNA were mainly responsible for the increasing PM_{2.5} pollution compared with organic matter (OM). NO₃⁻ was the most abundant species among water-soluble ions, but SO₄²⁻ played a much more important role in driving the elevated PM_{2.5} concentrations. The relative humidity (RH) and its precursor SO₂ were the key factors affecting the formation of sulfate. Homogeneous reactions dominated the formation of nitrate which was mainly limited by HNO₃ in ammonia-rich conditions. Secondary formation and regional transport from the heavily polluted region promoted the growth of PM_{2.5} concentrations in the formation stage of PM_{2.5} pollution in Beijing and Langfang. Regional transport or local emissions, along with secondary formation, made great contributions to the PM_{2.5} pollution in the evolution stage of PM_{2.5} pollution in Beijing and Langfang. The favourable meteorological conditions and regional transport from a relatively clean region both favored the diffusion of pollutants in all three cities.

© 2020 The Research Center for Eco-Environmental Sciences, Chinese Academy of Sciences. Published by Elsevier B.V.

* Corresponding authors.

E-mails: gaojian@cras.org.cn (J. Gao), zhongjunxu@163.com (Z. Xu).

Introduction

Severe PM_{2.5} (particles with an aerodynamic diameter less than 2.5 μm) pollution episodes have occurred frequently in recent years in China, especially during the heating season of the Beijing-Tianjin-Hebei (BTH) region (Chen et al., 2015; Gao et al., 2018). This problem has received substantial attention from the government, the public, and scientists due to its adverse effects on human health (Lu et al., 2015), visibility (Tian et al., 2016), and climate (Tai et al., 2010). Massive anthropogenic emission sources, as well as unfavorable geographical and meteorological conditions, resulted in the frequent occurrence of severe haze episodes with exceedingly high PM_{2.5} concentrations in the BTH region during the heating season (Fu and Chen, 2017; Wang et al., 2014).

Some studies on PM_{2.5} pollution in this region showed that secondary aerosol formation in the haze-fog events played a significant role in high PM_{2.5} levels in the winter (Han et al., 2014; Wang et al., 2015a). Zhao et al. (2013a) found that secondary inorganic ions (SNA, i.e., NO₃⁻+SO₄²⁻+NH₄⁺) caused approximately 30%-40% of winter PM_{2.5} in the BTH region. Other studies have investigated the formation mechanism of secondary inorganic ions in detail (Zheng et al., 2015; Quan et al., 2015). These studies concluded that high secondary inorganic ions concentrations in severe haze episodes could be ascribed to the heterogeneous reaction. Recent studies pointed out that NO_x promotion of SO₂ to sulfate conversion has become an important mechanism in heavy haze episodes in Beijing, due to the recent enhanced contributions of vehicle emissions (Ma et al., 2018; He et al., 2014). Efficient conversion of SO₂ to sulfate was not only conducive to the high sulfate production rate but also enhanced the formation of nitrate and secondary organic aerosols (SOAs) on aqueous particles (Wang et al., 2016). In addition, recent work has highlighted the importance of nitrate formation as the driving force of haze evolution during summer over the North China Plain (Li et al., 2018). Some scholars have also analyzed the cause of heavy pollution episodes in more detail. For example, Ji et al. (2014) found that the high local emissions under stagnant conditions were mainly responsible for the explosive growth in PM_{2.5} concentrations, and that a combination of slow regional transport and local accumulation favored consecutive increases in Beijing's PM_{2.5} concentrations in winter. For Tianjin, Han et al. (2014) contended that haze-fog pollution was mainly attributed to the high layer transport of the pollutants in the early period, as well as the late accumulation of pollutants and secondary aerosol formation in winter.

Most previous studies have focused on analyzing short-term haze events and seasonal variations in Beijing and Tianjin. However, the characteristics of chemical components have not been extensively investigated at multiple BTH sites over the full heating season. In addition, because many studies were mainly based on traditional 24-hr integrated filter-based measurements with low temporal resolution, they couldn't effectively capture the evolution progress of heavy pollution episodes. According to backward trajectories and the potential source contribution function (PSCF), the air quality of Beijing in winter is largely influenced by the regional transport from areas south and west of Beijing (Wang et al., 2015b). Therefore, in this study, chemical components in PM_{2.5} were simultaneously observed by online instruments with a 1-hr resolution in Beijing (the capital of China) and two adjacent southeast cities during the heating season: Tianjin (an economically developed municipality) and Langfang (a prefecture-level city in Hebei province). The primary purposes of this study are to (1) investigate the spatial characteristics of PM_{2.5} as well as its chemical compositions in the heating season, (2) explore the evolution of chemical compositions

in different pollution levels, (3) identify the difference in the formation mechanism of sulfate and nitrate, and (4) probe the formation mechanism of synchronized severe PM_{2.5} pollution episodes in all three cities.

1. Materials and methods

1.1. Measurement site and period

The observation campaign was conducted simultaneously in Beijing, Tianjin, and Langfang (Appendix A Fig. S1) from November 15, 2016 to March 15, 2017, the heating season in northern China. The observation site in Beijing was set up in a room approximately 10 m above the ground in the Chinese Research Academy of Environmental Sciences (CRAES) (116.40°E, 40.03°N), which is located in the urban downtown area of northern Beijing. It is representative of an urban district due to the mixed influence of residual, traffic, and construction emissions (Gao et al., 2016). The observation site in Tianjin was located on the rooftop of a building approximately 10 m above the ground in the Tianjin Environmental Monitoring Centre (117.15°E, 39.08°N), situated in the urban downtown of Tianjin. It is also considered to be representative of an urban district due to the mixed influence of residual and traffic emissions. The observation site in Langfang was situated on the rooftop of the Talent Exchange Centre (116.76°E, 39.57°N) in the Economic and Technological Development Zone, approximately 30 m above the ground. It is also representative of an urban district due to the mixed influence of residual, traffic, and industry emissions.

1.2. Sampling instrument

Mass concentrations of water-soluble inorganic ions (SO₄²⁻, NO₃⁻, NH₄⁺, Na⁺, K⁺, Cl⁻, Mg²⁺ and Ca²⁺) in Beijing were continuously measured at a 1-hr resolution by a model ADI 2080 online analyser (MARGA, model ADI 2080, Applikon Analytical B.V. Corp., Netherlands) equipped with a PM_{2.5} sampling inlet. The MARGA instrument consisted of a sampling box, an analytical box, and a control system. The sampling box was composed of a wet rotating denuder (WRD) as well as a steam jet aerosol collector (SJAR), which are used for absorbing water-soluble gases and capturing aerosol. Water-soluble inorganic ions' mass concentrations were detected using an automatic ion chromatography (IC) system in the analytical box. MARGA has been described in more detail in previous studies (Kong et al., 2018; Liu et al., 2017a). For detailed quality assurance/quality control (QA/QC) procedures, see Gao et al. (2016).

Two identical ambient ion monitors (Thermo Science URG 9000D, URG Corporation, USA) were used in Tianjin and Langfang to measure hourly mass concentrations of water-soluble ions (NH₄⁺, Na⁺, K⁺, Ca²⁺, Mg²⁺, SO₄²⁻, NO₃⁻, and Cl⁻) in PM_{2.5}. The instrument consisted of one particle collection unit and two IC analyzers for chemical analyses. The sample inlet was equipped with a PM_{2.5} sharp-cut cyclone operating at a flow rate of 3 L/min. The air was drawn through a liquid diffusion parallel-plate denuder that can separate the gas from the aerosol phase. The particle-laden air flow entered the particle supersaturation chamber to facilitate the particle hygroscopic growth into droplets to achieve high collection efficiencies. Then, the water-soluble components of the aerosol and gaseous phase were collected by four syringes installed into pre-concentrators and injected into the two ICs once per hour. Each analyzer (ICS-1100 Reagent Free, Dionex Corporation,

CA) was equipped with a guard column, an analytical column, and a self-regenerating suppressor. The water-soluble inorganic ions were analyzed in IC and quantified through an external standard method (Yuan et al., 2018). The relationships between the total anion equivalents and total cation equivalents in the three cities are shown in Appendix A Fig. S2. To further illustrate the accuracy of online measurement in the three cities, the concentrations of major chemical components such as SO_4^{2-} , NO_3^- , and NH_4^+ measured by the online analyzer were in good agreement with those measured by the offline filter method (Appendix A Fig. S3).

The organic carbon/elemental carbon (OC/EC) in aerosol in Beijing, Tianjin, and Langfang was measured by a field semi-online OC/EC analyzer (Model 4, Sunset Laboratory Inc., USA) with a $\text{PM}_{2.5}$ cyclone inlet. A carbon parallel-plate diffusion denuder was installed on the analyzer to remove volatile organic compounds (VOCs), which may cause a positive bias in the measured OC concentrations. The particulate samples were collected on quartz filters; the instrument operated at a flow rate of 8 L/min with a time resolution of 1-hr. The collected OC was evaporated, and after that it was oxidized to CO_2 either under the catalysis of MnO_2 or together with EC on the filter by oxygen in the He/O_x phase, and then the OC and EC were analyzed by a non-dispersive infrared (NDIR) detector. The detection limit of the semi-continuous OC/EC analyzer was 0.4 and 0.2 $\mu\text{g}/\text{m}^3$ for OC and EC, respectively.

The hourly $\text{PM}_{2.5}$, SO_2 , NO_2 , O_3 , and CO data were obtained from the website (<http://beijingair.sinaapp.com/>) from November 15, 2016 to March 15, 2017 in Beijing, Tianjin, and Langfang. Concentrations of $\text{PM}_{2.5}$ with 1-hr resolution from these sites also had a good relationship with those measured by the offline filter method during the heating season (Appendix A Fig. S3). The meteorological data, including wind direction, wind speed, temperature, precipitation, and relative humidity, were directly obtained from Institute of Beijing Urban Meteorology, China Meteorological Administration.

1.3. Aerosol liquid water content (ALWC) prediction from chemical composition

ISORROPIA-II is an efficient thermodynamic equilibrium model for the K^+ - Ca^{2+} - Mg^{2+} - NH_4^+ - Na^+ - SO_4^{2-} - NO_3^- - Cl^- - H_2O aerosol system, which can be used to predict aerosol liquid water content (ALWC). In this study, this model used the 'reverse' type in the metastable state with hourly concentrations of water soluble ions (K^+ , Ca^{2+} , Mg^{2+} , NH_4^+ , Na^+ , SO_4^{2-} , NO_3^- , and Cl^-), relative humidity (RH), and temperature (t) input to calculate the ALWC.

2. Results and discussion

2.1. Characteristics of $\text{PM}_{2.5}$

Hourly average $\text{PM}_{2.5}$ concentrations were $94.5 \pm 108.5 \mu\text{g}/\text{m}^3$ in Beijing, $111.5 \pm 98.5 \mu\text{g}/\text{m}^3$ in Tianjin, and $106.4 \pm 97.9 \mu\text{g}/\text{m}^3$ in Langfang, respectively, during the heating season. Hourly $\text{PM}_{2.5}$ concentrations varied widely, with a range of 3–713, 1–559, and 5–464 $\mu\text{g}/\text{m}^3$ (Appendix A Fig. S4), respectively. The maximum hourly $\text{PM}_{2.5}$ concentrations were recorded at 5:00 am and 1:00 am on January 28 (the Chinese Lunar New Year), in Beijing and Langfang, respectively, which could be ascribed to fireworks burning (Yang et al., 2014). The proportion of daily average $\text{PM}_{2.5}$ concentrations over 75 $\mu\text{g}/\text{m}^3$ (Grade II National Ambient Air Quality Standard, GB3095-2012) throughout the entire observation period was 44.6%, 56.2%, and 51.2% in Beijing, Tianjin, and Langfang. Severe $\text{PM}_{2.5}$ pollution episodes occurred frequently and synchronously in

Table 1 – Mean mass concentrations of chemical components in the heating season in Beijing, Tianjin and Langfang ($\mu\text{g}/\text{m}^3$).

Species	Beijing	Tianjin	Langfang
NO_3^-	15.8±16.9	14.6±14.0	18.2±18.2
SO_4^{2-}	11.9±14.5	11.9±12.5	15.0±15.5
NH_4^+	11.1±13.7	10.0±8.4	12.1±12.1
Cl^-	4.4±4.6	4.2±4.1	4.8±4.4
K^+	2.9±7.2	1.6±2.4	1.4±1.3
Na^+	0.6±0.4	0.8±0.5	1.3±0.6
Ca^{2+}	0.7±0.5	0.3±0.2	0.6±0.5
Mg^{2+}	0.6±1.0	0.1±0.2	0.3±0.6
OC	15.2±14.6	18.9±13.5	23.7±20.9
EC	6.3±5.6	5.7±5.1	7.6±7.3
SNA	41.6±44.3	37.1±34.6	46.2±45.6
SNA/ $\text{PM}_{2.5}$	34.9%±11.7%	30.4%±10.9%	37.9%±12.7%

OC: organic carbon; EC: elemental carbon; SNA: SO_4^{2-} , NO_3^- , and NH_4^+ ; $\text{PM}_{2.5}$: particles with an aerodynamic diameter less than 2.5 μm .

all three cities. Here, we define a pollution episode (EP) as a set of continuous days with daily $\text{PM}_{2.5}$ mass concentrations over 75 $\mu\text{g}/\text{m}^3$. There were approximately twelve severe $\text{PM}_{2.5}$ pollution episodes happening synchronously in these three cities (Appendix A Fig. S5). $\text{PM}_{2.5}$ concentrations during these pollution episodes were 4.9–5.9 times as high as that on clean days ($\text{PM}_{2.5} < 75 \mu\text{g}/\text{m}^3$). As was mentioned above, these results illustrate the seriousness of fine particle pollution on a regional scale. In order to get more insights into $\text{PM}_{2.5}$ pollution situations in the three cities, $\text{PM}_{2.5}$ concentrations were compared across different cities in China and in foreign countries, and the results are presented in Appendix A Table S1. It was found that the $\text{PM}_{2.5}$ pollution in different regions has its own temporal and spatial characteristics. Average ratios of $\text{PM}_{2.5}/\text{PM}_{10}$ were used to determine differences in particle size fractions. The $\text{PM}_{2.5}/\text{PM}_{10}$ ratios were $63.6\% \pm 24.8\%$ in Beijing, $69.4\% \pm 22.1\%$ in Tianjin, and $64.1\% \pm 16.5\%$ in Langfang. These are very consistent with the values 60%–70% calculated in winter in Northern China (Xu et al., 2017; Shao et al., 2018).

2.2. Characteristics of chemical components

2.2.1. Water-soluble ions

Table 1 shows the average concentrations and ratios of chemical components in $\text{PM}_{2.5}$. The fraction of SNA in $\text{PM}_{2.5}$ was around 30%–40% in the three cities. Xu et al. (2019) also reported that SNA comprised approximately 20%–40% of $\text{PM}_{2.5}$ during winter in the BTH region. However, although a high fraction of SNA in $\text{PM}_{2.5}$ was observed in winter, the season with the highest SNA fraction was summer, due to strong photochemical reactions, as reported by many studies in Beijing and Tianjin (Gao et al., 2016; Huang et al., 2017). The ratio of $\text{NO}_3^-/\text{PM}_{2.5}$ among the water-soluble ions was the highest in Beijing 14.0% ± 6.3%, Tianjin 11.6% ± 5.5% and Langfang 15.7% ± 6.2%, reflecting the dominant role of NO_3^- in water-soluble ions. However, in previous studies SO_4^{2-} was identified as the dominant ion in winter, in both Beijing and Tianjin (Cao et al., 2012; Song et al., 2007; Li et al., 2009; Gu et al., 2011). The decline in SO_4^{2-} concentrations in recent years may be related to the dramatic reduction in SO_2 emissions due to strict control measures (Li et al., 2017). The $\text{NO}_3^-/\text{SO}_4^{2-}$ mass ratio was generally used to gain some insights regarding the relative contributions of mobile versus stationary sources in the atmosphere (Arimoto et al., 1996). The $\text{NO}_3^-/\text{SO}_4^{2-}$ ratio

was greater than 1.0, suggesting that the mobile source emissions might be predominant in three cities. These ratios were apparently higher than those in many other cities in China (Appendix A Table S2). These results clearly reveal the seriousness of nitrate pollution, which was largely influenced by increasing motor vehicle emissions, and highlight the importance of controlling NO_x emissions. It is noteworthy that the $\text{NO}_3^-/\text{SO}_4^{2-}$ mass ratio was lower than 1.0 before the 2010 winter in Beijing, while the increase in the $\text{NO}_3^-/\text{SO}_4^{2-}$ mass ratio in recent years was likely related to the increases in motor vehicles.

2.2.2. OC and EC

The total carbon (TC, calculated by the sum of OC and EC) constituted 26.5%–30.1% of $\text{PM}_{2.5}$ in these three cities, which is consistent with previous studies (10%–30%) in other Chinese cities (Qiu et al., 2016; Wang et al., 2015c). The average OC/EC mass ratios were 2.9 in Beijing, 4.7 in Tianjin, and 3.7 in Langfang, all of which agreed well with the OC/EC mass ratio (2–6) in many megacities in China (Gu et al., 2010).

To better estimate the secondary organic carbon (SOC) contribution to OC, the EC-tracer method (Hu et al., 2012) is widely used to calculate SOC concentration, based on the following equation:

$$\text{SOC} = \text{OC}_{\text{tot}} - \text{EC} \times (\text{OC/EC})_{\text{pri}} \quad (1)$$

where OC_{tot} is the total OC and $(\text{OC/EC})_{\text{pri}}$ is the primary OC/EC ratio, which is usually estimated by the data pairs with the lowest 10% percentile of ambient OC/EC ratios (Zheng et al., 2015). The slope of the regression line from data pairs was used to identify $(\text{OC/EC})_{\text{pri}}$ (Chu, 2005). The average SOC concentrations were 6.4 ± 6.3 , 5.1 ± 3.1 and 5.5 ± 5.6 $\mu\text{g}/\text{m}^3$, with contributions of 37.1% \pm 16.9%, 36.3% \pm 20.7%, and 29.2% \pm 15.8% to OC, respectively, in Beijing, Tianjin, and Langfang. This illustrates that primary organic carbon (POC) was the main contributor to OC in all three cities. Some studies have also concluded that the formation of SOC had a minor impact on the accumulation of OC, instead arguing that POC was mainly responsible for the enhanced OC in the Beijing-Tianjin-Hebei region (Yang et al., 2018; Zhao et al., 2013b; Lin et al., 2009). Although stagnant air, high RH, and low temperature may exert a strong influence on the gas-to-particle partitioning of semi-volatile organic compounds in the heating season (Zhang et al., 2015), the contribution of SOC to $\text{PM}_{2.5}$ was somewhat less significant than POC.

2.3. Chemical components in different pollution conditions

We classified $\text{PM}_{2.5}$ -polluted conditions into four categories based on the Air Quality Index: clean (C) ($\text{PM}_{2.5} < 75$ $\mu\text{g}/\text{m}^3$), slight pollution (S) (75 $\mu\text{g}/\text{m}^3 \leq \text{PM}_{2.5} < 150$ $\mu\text{g}/\text{m}^3$), moderate pollution (M) (150 $\mu\text{g}/\text{m}^3 \leq \text{PM}_{2.5} < 250$ $\mu\text{g}/\text{m}^3$), and heavy pollution (H) ($\text{PM}_{2.5} \geq 250$ $\mu\text{g}/\text{m}^3$). Fig. 1 shows the variations in chemical components of $\text{PM}_{2.5}$ in each city. Chemical composition was dominated by organic matter (OM = OC \times 1.6) (Turpin and Lim, 2001) in C conditions, followed by SNA in Tianjin and Langfang. However, in Beijing the contribution of OM to chemical composition was comparable to SNA in C conditions. SNA obviously exhibited higher concentrations than OM in the S, M, and H conditions in each city. Although the mass concentrations of SNA, OM, and EC all showed increases at different paces with aggravating pollution, the relative contributions of these chemical compositions varied in different ranges. The contribution of SNA to chemical composition increased gradually as the pollution levels increased in each city. In particular, the fraction of SNA in H conditions

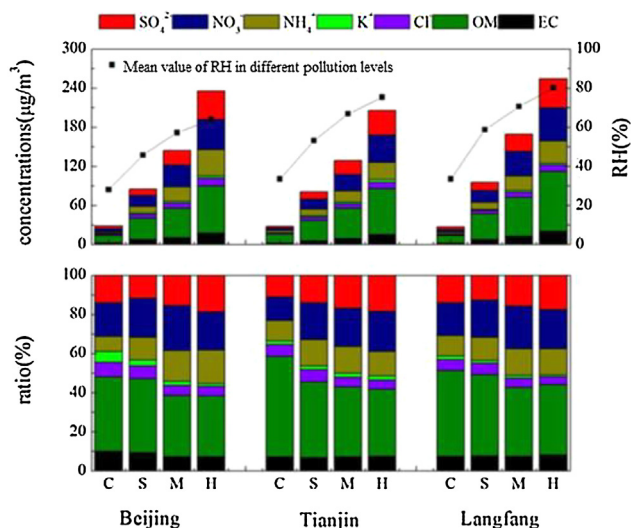


Fig. 1 – Concentrations and Ratio of the chemical components in different pollution levels in Beijing, Tianjin and Langfang. C: clean; S: slight pollution; M: moderate pollution; H: heavy pollution; RH: relative humidity; OM: organic matter.

reached 50%–55%. However, the contribution of OM showed a gradually decreasing trend as the $\text{PM}_{2.5}$ pollution evolved. These results reflect that SNA had a much more substantial influence on driving elevated $\text{PM}_{2.5}$ concentrations.

It is noteworthy that the percentage of NO_3^- decreased from 23.1% to 19.5% in Beijing, increased slightly from 19.6% to 20.4% in Tianjin, and declined from 21.9% to 19.9% in Langfang from M to H conditions. In contrast to the contribution of NO_3^- to chemical composition, SO_4^{2-} showed a greater increase in its fraction, increasing from 15.4% to 18.7% in Beijing, from 16.7% to 18.2% in Tianjin, and from 15.8% to 17.5% in Langfang. Overall, the significant increase in the fraction of SO_4^{2-} suggests that the elevated $\text{PM}_{2.5}$ concentrations were largely driven by SO_4^{2-} . This reason might be that the high RH were in favor of the heterogeneous reaction of sulfate with the increase of $\text{PM}_{2.5}$ pollution (Fig. 1). The formation mechanism of sulfate and nitrate would be illustrated in detail in the following.

2.4. Conversion from gas to particle phase

The sulfur oxidation ratio, defined as $\text{SOR} = n\text{-NSS-SO}_4^{2-}/(n\text{-NSS-SO}_4^{2-} + n\text{-SO}_2)$, and the nitrogen oxidation ratio, defined as $\text{NOR} = n\text{-NO}_3^-/(n\text{-NO}_3^- + n\text{-NO}_2)$, are used to evaluate the degree of secondary conversion (Yang et al., 2018). Here, n refers to the molar concentration and NSS refers to non-sea salt. NSS-SO_4^{2-} was estimated with the following equation in Tianjin (Morales et al., 1998):

$$\text{NSS-SO}_4^{2-} = [\text{SO}_4^{2-}] - 0.2455[\text{Na}^+] \quad (2)$$

The average SOR was 0.30 ± 0.11 , 0.21 ± 0.14 , and 0.32 ± 0.19 in Beijing, Tianjin, and Langfang, respectively. The average NOR was 0.11 ± 0.08 , 0.12 ± 0.08 , and 0.14 ± 0.08 , respectively. Fig. 2 shows the variations of SOR, NOR, $\text{SO}_4^{2-}/\text{EC}$, and NO_3^-/EC in different pollution conditions in the three cities. $\text{SO}_4^{2-}/\text{EC}$ and NO_3^-/EC were used to exclude the effect

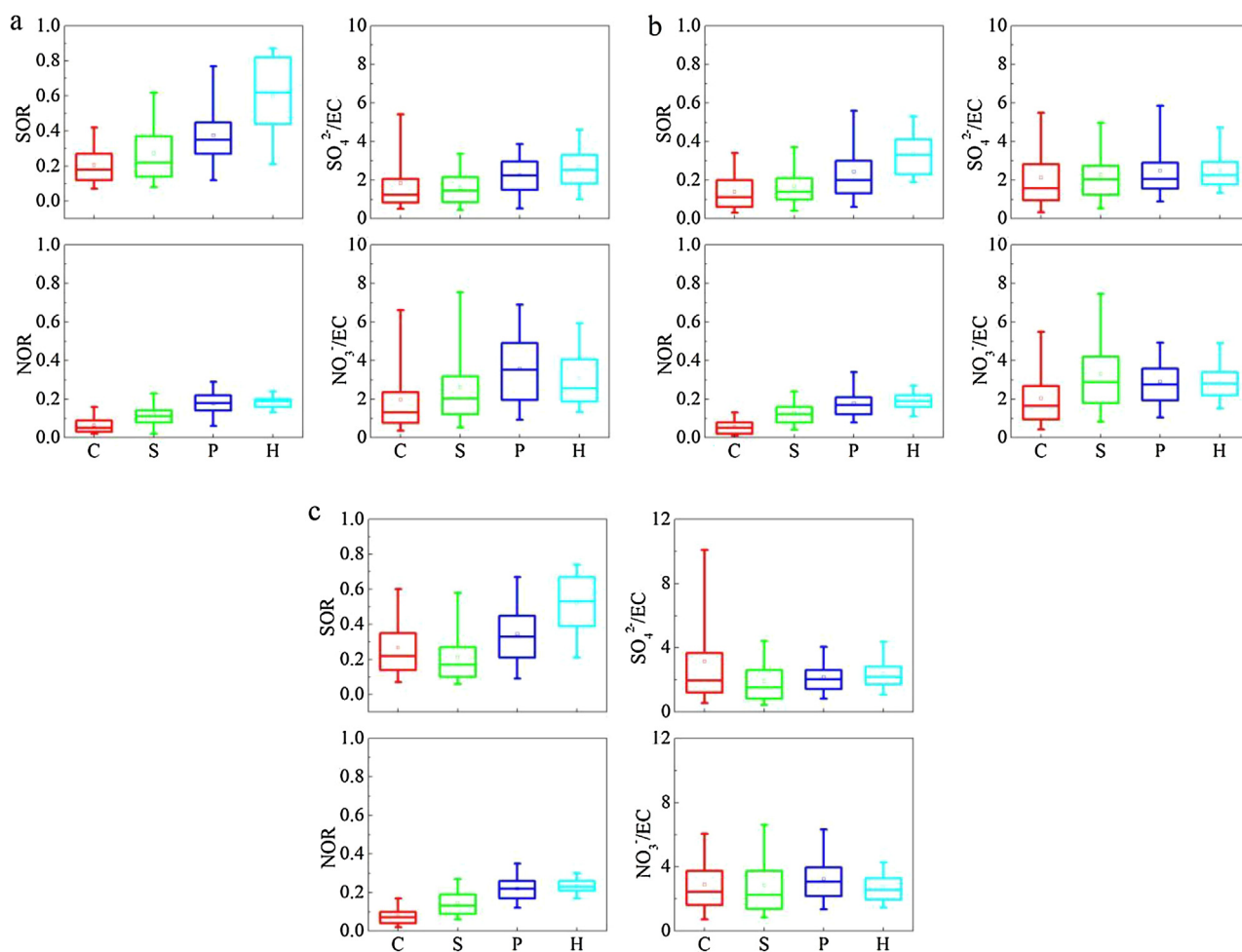


Fig. 2 – Variations of sulfur oxidation ratio (SOR), nitrogen oxidation ratio (NOR), $\text{SO}_4^{2-}/\text{EC}$ and NO_3^-/EC with pollution levels in (a) Beijing, (b) Tianjin and (c) Langfang. In the box-whisker plots, the whiskers and boxes indicated the 95th, 75th, 50th (median), 25th and 5th percentiles, respectively. The small box inside every box-whisker plot was the mean value.

of different dilution/mixing conditions on the variation of observed pollutant concentrations (Zheng et al., 2015). The highest SOR was found in H conditions, with variations up to factors of 2.9, 2.4, and 1.9 compared with C conditions. The variation trend of $\text{SO}_4^{2-}/\text{EC}$ was similar to SOR in all three cities. For example, $\text{SO}_4^{2-}/\text{EC}$ and $\text{NSS-SO}_4^{2-}/\text{EC}$ evidently rose from C to H in Beijing and in Tianjin. $\text{SO}_4^{2-}/\text{EC}$ exhibited a similar pattern with SOR, which also dropped first and then increased in Langfang. These results clearly reveal the enhanced secondary transformation of SO_2 as $\text{PM}_{2.5}$ pollution is aggravated. Even though NO_3^- concentrations increased by factors of approximately 8–12 from C to H conditions in all three cities, NOR showed no similar increasing trend. This suggests that SO_2 is more easily oxidized than NO_2 .

The variations between SOR and RH in different pollution conditions in Beijing, Tianjin, and Langfang are shown in Appendix A Fig. S6. The heterogeneous reaction was too weak to be considered when RH was less than 30%, due to extremely low particle phase water (Khoder, 2002). SOR kept increasing rapidly with the escalation of RH when RH was greater than 30% under C, S, M, and H conditions in all three cities. This result demonstrates the crucial effects of RH on the formation of sulfate. Water vapor is easily absorbed by the surface

of the particulate matter at higher RH levels, especially in the presence of H_2O_2 or a metal oxidant, so more SO_2 will be absorbed, further accelerating the heterogeneous reaction of sulfate (Seinfeld and Pandis, 2006). However, SOR experienced a significant decreasing trend with RH increasing when RH was lower than 40% in C conditions, possibly due to the photochemical reaction of SO_2 . Considering that sulfate is also formed through the gas-phase oxidation of SO_2 by OH and H_2O_2 (Xue et al., 2016), and O_3 plays an important role in atmospheric chemistry because it acts as an important source of OH radicals through photolysis (Du et al., 2011). The relationship between SOR and O_3 could be used to confirm the impacts of photochemical reactions on the formation of sulfate.

Under exacerbating pollution, high particle matter concentrations in the troposphere would hinder amounts of the solar radiation from reaching the ground (Tian et al., 2014), thereby resulting in the reduction of the photochemical reaction. Under this circumstance, especially in H conditions, lower O_3 concentrations (Appendix A Fig. S7) were observed, which made it difficult for the gas-phase reaction of sulfate formation. There was no particularly evident increasing trend for the variations of SOR with O_3 in other pollution conditions (Appendix A Fig. S7), suggesting that the heterogeneous reac-

tion has a greater effect on the formation of sulfate compared with the photochemical reaction. However, SOR progressively increased as O_3 increased in C conditions, suggesting a relatively significant influence of high O_3 concentrations on the photochemical reaction of SO_2 . CO is also regarded as a good tracer that could be used to eliminate the influence of meteorological factors on the variation of observed pollutant concentrations (Liu et al., 2019). It is worth noting that SOR displayed a decreasing trend with the growth of CO-scaled SO_2 concentrations and that SOR presented a higher value under high RH conditions (Appendix A Fig. S8), which may be related to more conversion of SO_2 involving the formation of sulfate under higher RH conditions (Shao et al., 2018). Thus, it can be concluded that RH and SO_2 were important factors in the formation of sulfate during pollution conditions in all three cities.

The variations of NOR with RH in different pollution conditions in Beijing, Tianjin, and Langfang are shown in Appendix A Fig. S9. The NOR maintained no sharp increase with increasing RH in clean and pollution conditions in each city. This result shows that RH has become a more vital contributing factor to the formation of sulfate than that of nitrate. Nitrate can be formed through reactions between the ambient ammonia and nitric acid (Pathak et al., 2009). Nitric acid can be formed by two important paths: one through the homogeneous reaction of NO_2 and OH radicals during the day, and the other by heterogeneous reactions through the hydrolysis of N_2O_5 on the pre-existing aerosols at night (Seinfeld and Pandis, 2006). The “Excess NH_4^+ ” was defined as the amount of ammonium in excess of that needed for $[NH_4^+]/[SO_4^{2-}] = 1.5$ (i.e., $[NH_4^+]_{\text{Excess}} = ([NH_4^+]/[SO_4^{2-}] - 1.5) \times [SO_4^{2-}]$; note that [X] denotes molar concentrations ($\mu\text{mol}/\text{m}^3$) of the species X). If “Excess NH_4^+ ” was greater than 0, the area was considered ammonium-rich; otherwise, it was regarded as ammonium-poor (Pathak et al., 2009). The $[NH_4^+]_{\text{Excess}}$ values were always more than 0, suggesting that Beijing, Tianjin, and Langfang were in ammonia-rich conditions. The $[NH_4^+]_{\text{Excess}}$ was also linearly correlated with $[NO_3^-]$ in clean and pollution conditions in all three cities (Appendix A Fig. S10), indicating that nitrate aerosols began to form when $[NH_4^+]/[SO_4^{2-}]$ was more than 1.5.

Diurnal variations of NOR, NO_3^-/CO , NO_2/CO , O_3 , RH, and t (temperature) in Beijing, Tianjin, and Langfang are shown in Appendix A Fig. S11. The diurnal trends of NOR demonstrated that NOR exhibited a strong O_3 concentration dependency during the day and reached its peak in the afternoon, around 14:00 to 16:00 in each city, as shown in Appendix A Fig. S11. The NO_3^-/CO increased continuously during the day and presented a significant peak at RH around 30%–40% at 16:00. The NO_2/CO varied in a low-level range during the day, along with the increase in NO_3^-/CO . Therefore, the heterogeneous reaction of NO_2 seems unlikely to be an important pathway of nitrate formation during the day due to low RH. Instead, the photochemical reactions were mainly responsible for the formation of daytime nitrate due to high O_3 concentrations. Although NOR had relatively low values in Beijing, Tianjin, and Langfang at night, it also showed an increasing trend, suggesting the pronounced role of the heterogeneous hydrolysis of N_2O_5 in the formation of nitrate. As mentioned above, the formation of nitrate was mainly limited by HNO_3 in the ammonium-rich atmosphere in all three cities. Thus, more control measures should be focused on the NO_2 and O_3 emissions. In a word, the photochemical reactions played a much more significant role in the formation of nitrate than sulfate, and the heterogeneous reactions had a greater impact on the formation of the sulfate compared with nitrate.

2.5. Formation mechanism of heavy $PM_{2.5}$ pollution episodes in the heating season

To further illustrate the effect of secondary formation in $PM_{2.5}$ pollution, a long-lasting heavy regional pollution episode was selected to explore the effect in detail. The formation mechanism of $PM_{2.5}$ pollution is very complex, and is also affected by meteorological conditions, source emissions, and regional transport (Duan et al., 2019; Liu et al., 2017b), which necessitates further discussion of its causes. A long-lasting heavy regional pollution episode occurred concurrently in Beijing, Tianjin, and Langfang from December 29, 2016 to January 9, 2017, with daily average $PM_{2.5}$ concentrations reaching 203.0, 192.1, and 208.9 $\mu\text{g}/\text{m}^3$, i.e., 2.7, 2.6, and 2.8 times higher than 75 $\mu\text{g}/\text{m}^3$, respectively (Fig. 3). We demonstrated that the evolution of this heavy $PM_{2.5}$ pollution episode (EP) consisted of three stages: (1) EP1 (a formation stage), (2) EP2 (an evolution stage) and (3) EP3 (a clearing stage).

In EP1, $PM_{2.5}$ concentrations presented similar variation characteristics in all three cities. The $PM_{2.5}$ concentration gradually accumulated, peaking on January 1, December 31, and December 31 to the level of 458, 327, and 327 $\mu\text{g}/\text{m}^3$, respectively in Beijing, Tianjin and Langfang. On this day, the prevailing wind was from the southwest with low wind speed (~ 2 m/sec) in the region. Ma et al. (2017) also reported that $PM_{2.5}$ concentration rapidly increased to the haze pollution level in Beijing when the wind direction changes to southerly. Considerable amounts of pollutants were brought to this region by the southerly winds. Forty-eight hour back trajectories were calculated by the National Oceanographic and Atmospheric Administration (NOAA) HYSPLIT model to interpret the origin and transport pathway of the air masses arriving at these cities (Appendix A Figs. S12, S13, and S14). The backward trajectory of the air mass at altitudes of 1000 and 500 m could be used to demonstrate the impacts of regional transport on coarse particles (Yang et al., 2015) during this heavy pollution episode, so the air mass at an altitude of 100 m was used to analyze the influence of regional transport on $PM_{2.5}$ pollution. As $PM_{2.5}$ levels increased, the air mass transported into the region changed gradually, changing to a southwest wind from the original north-northwest wind. The considerable mixed pollutants emitted from the southwestern part of the region where located amounts of industries could be transported into the region, further exacerbating $PM_{2.5}$ pollution in the region (Gao et al., 2015).

Cl^- , K^+ , NO_3^- , SO_4^{2-} , NH_4^+ , OC, and EC in Beijing increased by factors of 6.2, 1.5, 4.9, 9.7, 9.0, 1.1, and 2.0, respectively. It was evident that the enhanced factor of SO_4^{2-} was the highest, and Cl^- , SO_4^{2-} , and NH_4^+ were the three major water-soluble ions mainly responsible for the elevated $PM_{2.5}$ levels. During this period, SOR increased from 0.20 to 0.85, while the SO_4^{2-} fraction in $PM_{2.5}$ was elevated from 12.1% to 15.3% in Beijing as RH increased from 30.2% to 77.8%, which may be related to the crucial impacts of heterogeneous reactions on the formation of sulfate. The water-soluble ions, OC and EC data in Tianjin were insufficient to calculate the enhanced factors there. Chemical components were characterized by high enhanced factors of SO_4^{2-} (5.9), K^+ (5.7), and Cl^- (4.5) in Langfang. Note that SO_4^{2-} also presented the highest enhanced factor in Langfang. K^+ was considered as the tracer of biomass burning (Watson et al., 2001). It was suggested that $PM_{2.5}$ was largely under the influence of biomass burning. Cl^- was usually from coal combustion (He et al., 2001). The obvious increase in SOR was from 0.23 to 0.65, along with the significant increase in SO_4^{2-} fraction in $PM_{2.5}$ (from 10.5% to 17.4%), was also accompanied by a rising RH (from 37.9%

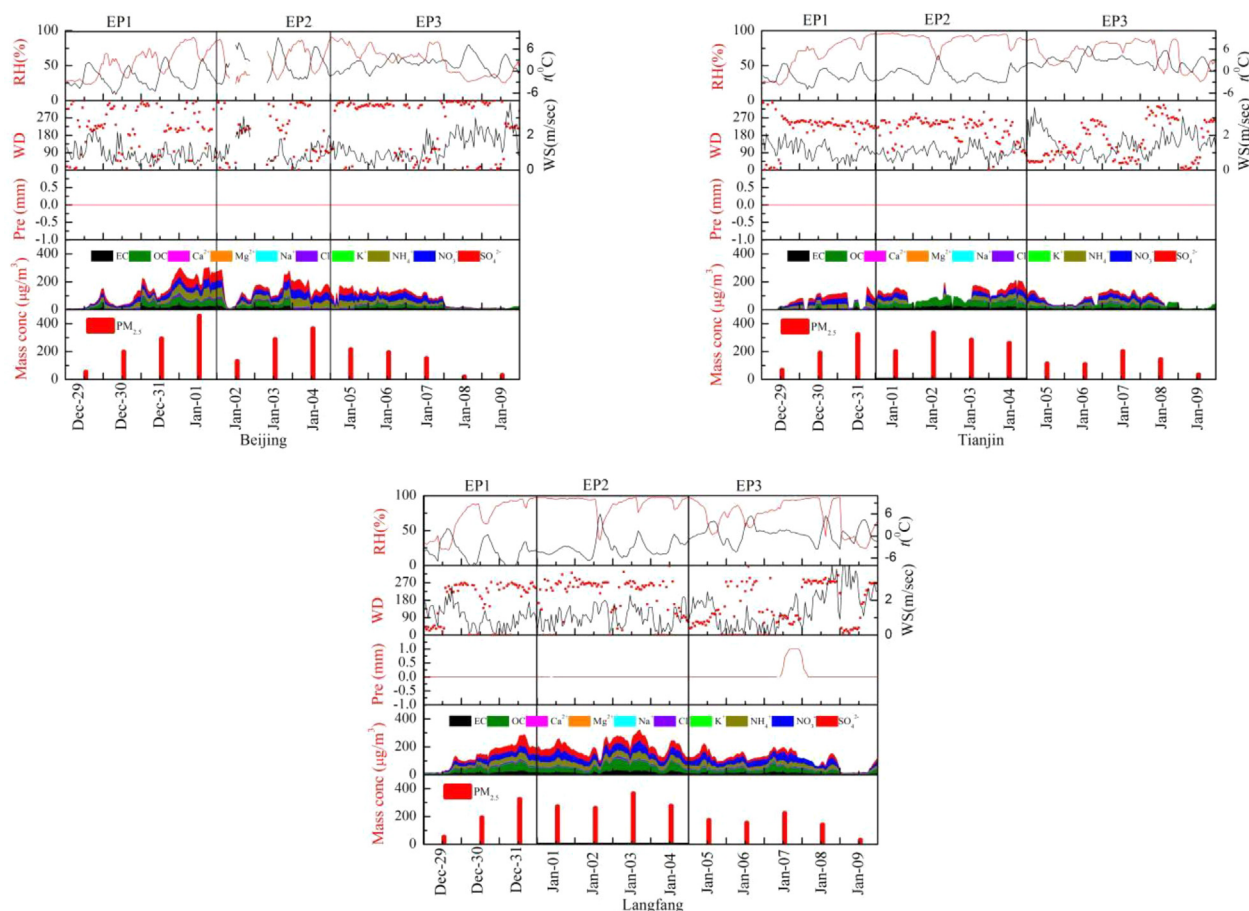


Fig. 3 – Time series of daily $PM_{2.5}$ concentrations, relevant parameters and chemical components in a heavy pollution episode (EP) in Beijing, Tianjin and Langfang. conc: concentrations; WD: wind direction; Pre: precipitation; WS: wind speed; t: temperature.

to 92.4%), suggesting that heterogeneous reactions played a significant role in the formation of sulfate in Langfang.

In stage EP2, $PM_{2.5}$ concentrations maintained a relatively high level in all three cities. The southwest wind with low wind speed (~ 2 m/sec) was still the dominant wind in the region. The air masses on January 1 in Tianjin and Langfang, and on January 3 in all three cities, passed over southwest regions which had massive anthropogenic emissions before reaching these three cities, which could facilitate the accumulation of pollutants. The long-range air masses on January 2 in Beijing and on January 4 in all three cities passed over Inner Mongolia and northern Hebei. Thus, the contribution of local emission sources was dominant due to the relatively low emission levels in the northwest of the region (Wang et al., 2018). The medium-long range air masses originated from west Inner Mongolia where there are large amounts of industrial activities and intense population (Ji et al., 2019), thus bringing massive pollutants into this region on January 2 in Tianjin and Langfang.

During this stage, SNA was the dominant contributor to $PM_{2.5}$, followed by OM, in Beijing and Langfang. The ranking of the mass concentration was $NO_3^- > SO_4^{2-} > NH_4^+$ in Beijing, but $SO_4^{2-} > NO_3^- > NH_4^+$ in Langfang. However, the concentrations of SO_4^{2-} from 22:00 on January 3, 2017 to 10:00 on January 4, 2017 were significantly higher than that of NO_3^- in Beijing. During this period, RH stayed at high levels and SOR was around 0.57–0.84 (Appendix A Fig. S15).

These results reveal that high RH levels have much more important impacts in the formation of sulfate than nitrate in Beijing. Three growth episodes were observed in Beijing and Langfang (Appendix A Table S3). ALWC served as a medium for heterogeneous reactions, and influenced the partitioning of gas-phase water soluble organic compounds to the condensed phase (Bian et al., 2014; Hennigan et al., 2008), resulting in visibility degradation (Deng et al., 2016). The SNA data in Tianjin is insufficient to calculate the concentrations of SNA and their contribution to $PM_{2.5}$. OM concentrations were $68.8 \pm 21.0 \mu\text{g}/\text{m}^3$ and contributed to $24.6\% \pm 7.5\%$ of $PM_{2.5}$ in Tianjin. SOC concentrations were 8.8 ± 4.7 , 4.7 ± 3.2 , and $5.5 \pm 3.6 \mu\text{g}/\text{m}^3$, and the SOC/OC ratio was only $29.5\% \pm 7.0\%$, $11.9\% \pm 7.9\%$, and $13.7\% \pm 7.2\%$, respectively, in Beijing, Tianjin, and Langfang. High particle concentrations in the troposphere weakened the solar radiation, reducing the generation of SOC due to the low atmospheric oxidation capability of organic matter (Tian et al., 2014).

In stage EP3, $PM_{2.5}$ concentrations gradually dropped in all three cities. The variation of $PM_{2.5}$ in Tianjin and Langfang showed similar characteristics in that $PM_{2.5}$ reached a high value on January 7. The low precipitation (~ 1 mm) on January 7 and 8 in Langfang did not effectively scavenge $PM_{2.5}$ concentrations, so the concentration of $PM_{2.5}$ remained at a high level. The prevailing wind was from the northwest direction in Beijing, but from the northeast in Tianjin and Langfang. All three cities experienced a higher wind speed (> 2 m/sec) with

the decrease of PM_{2.5} concentrations. As PM_{2.5} levels reduced, air masses transported into the region changed gradually, changing to a north and a north-northwest region (a relatively clean area in the BTH region due to less industry emission) from the original southwest, southeast, and south regions.

During this stage, SNA concentrations were higher than OM concentrations in each city. The mass concentration followed the order of NO₃⁻ > SO₄²⁻ > NH₄⁺ in each city. The fraction of NO₃⁻ in PM_{2.5} was greater than that of SO₄²⁻ with decreasing PM_{2.5} pollution. RH was lower in Stage EP3 than in Stage EP2. This suggests that sulfate was more sensitive to the reduction of RH than nitrate as the pollution levels decreased. Although SOC concentrations in Stage EP3 (4.7 ± 2.1, 3.6 ± 2.1, and 5.4 ± 3.3 μg/m³, respectively) were lower than that in Stage EP2, the ratio of SOC/OC was higher than in Stage EP2, which accounted for 43.1% ± 24.4%, 23.5% ± 13.8%, and 21.4% ± 11.5% of PM_{2.5}, respectively. Photochemical activities may contribute to the formation of SOC due to elevated O₃ concentrations (Appendix A Fig. S15).

3. Conclusions

The characteristics of chemical components and PM_{2.5} pollution evolution processes were investigated in detail during the 2016–2017 heating season in Beijing, Tianjin, and Langfang. The following conclusions were made.

- (1) The SNA dominated water-soluble ions, constituting around 30%–40% of PM_{2.5}. The mean mass ratio of NO₃⁻/SO₄²⁻ was more than 1.0, demonstrating that a mobile source might be a dominant contributor to PM_{2.5} in all three cities. The TC presented a contribution to approximately 26.5%–30.1% of PM_{2.5}. Low SOC/OC ratios (~40%) in all three cities implied that the formation of SOC wasn't conducive to the OC accumulation and that POC was primarily responsible for the enhanced OC.
- (2) The variations in the concentrations and ratios of chemical components at different pollution levels in all three cities show that OM almost dominated chemical components in clean conditions and SNA has the higher contribution in pollution conditions. With the aggravation of pollution, the fraction of SO₄²⁻ showed significant increase, which was due to the heterogeneous reaction of sulfate.
- (3) Regional transport and secondary formation were responsible for the growth of PM_{2.5} in the formation stage of PM_{2.5} pollution in Beijing and Langfang. Regional transport or local emissions, along with secondary formation, promoted consecutive increases in PM_{2.5} in the evolution stage of pollution in Beijing and Langfang. Favorable meteorological conditions and the regional transport from a relatively clean region facilitated the diffusion of pollutants in the clearing stage in all three cities.

Declaration of competing interest

The authors declare that they have no known competing financial interests or personal relationships that could have appeared to influence the work reported in this paper.

Acknowledgments

This study is supported by the National Natural Science Foundation of China (No. 91544226), the National Key Research and Development Plan of China (Nos. 2017YFC0209503 and

2016YFC0206202), and the National Research Program for Key Issues in Air Pollution Control in China (No. DQGG0107-03). The author is grateful to the financial support from CSC (Chinese Scholarship Council). The author thanks Lidia Morawska Professor for providing me with a good learning atmosphere when I was in the International Laboratory for Air Quality and Health (ILAQH) at Queensland University of Technology (QUT). We also thanks Environmental Monitoring Centers at Tianjin and Langfang for their contributions on the field measurements.

Appendix A. Supplementary data

Supplementary material associated with this article can be found in the online version at doi:10.1016/j.jes.2020.03.024.

REFERENCES

- Arimoto, R., Duce, R.A., Savoie, D.L., Prospero, J.M., Talbot, R., Cullen, J.D., et al., 1996. Relationships among aerosol constituents from Asia and the North Pacific during PEM-West A. *J. Geophys. Res.* 101, 2011–2023.
- Bian, Y.X., Zhao, C.S., Ma, N., Chen, J., Xu, W.Y., 2014. A study of aerosol liquid water content based on hygroscopicity measurements at high relative humidity in the North China Plain. *Atmos. Chem. Phys.* 14 (12), 6417–6426.
- Cao, J.J., Shen, Z.X., Chow, J.C., Watson, J.G., Lee, S.C., Tie, X.X., et al., 2012. Winter and summer PM_{2.5} chemical/compositions in fourteen Chinese cities. *J. Air Waste Manage. Assoc.* 62, 1214–1226.
- Chen, H.S., Li, J., Ge, B.Z., Yang, W.Y., Wang, Z.F., Huang, S., et al., 2015. Modeling study of source contributions and emergency control effects during a severe haze episode over the Beijing-Tianjin-Hebei area. *Sci. China. Chem.* 58 (9), 1403–1415.
- Chu, S.H., 2005. Stable estimate of primary OC/EC ratios in the EC tracer method. *Atmos. Environ.* 39 (8), 1383–1392.
- Deng, H., Tan, H.B., Li, F., Cai, M.F., Chan, P.W., Xu, H.P., et al., 2016. Impact of relative humidity on visibility degradation during a haze event: a case study. *Sci. Total Environ.* 569, 1149–1158.
- Du, H.H., Kong, L.D., Cheng, T.T., Chen, J.M., Du, J.F., Li, L., et al., 2011. Insights into summertime haze pollution events over Shanghai based on online water-soluble ionic composition of aerosols. *Atmos. Environ.* 45 (29), 5131–5137.
- Duan, J., Huang, R.J., Lin, C.S., Dai, W.T., Wang, M., Gu, Y.F., et al., 2019. Distinctions in source regions and formation mechanisms of secondary aerosol in Beijing from summer to winter. *Atmos. Chem. Phys.* 19 (15), 10319–10334.
- Fu, H.B., Chen, J.M., 2017. Formation, features and controlling strategies of severe haze-fog pollutions in China. *Sci. Total Environ.* 578, 121–138.
- Gao, J., Peng, X., Chen, G., Xu, J., Shi, G.L., Zhang, Y.C., et al., 2016. Insights into the chemical characterization and sources of PM_{2.5} in Beijing at a 1-h time resolution. *Sci. Total Environ.* 542, 162–171.
- Gao, J.J., Wang, K., Wang, Y., Liu, S.H., Zhu, C.Y., Hao, J.M., et al., 2018. Temporal-spatial characteristics and source apportionment of PM_{2.5} as well as its associated chemical species in the Beijing-Tianjin-Hebei region of China. *Environ. Pol.* 233, 714–724.
- Gao, J.J., Tian, H.Z., Cheng, K., Lu, L., Zheng, M., Wang, S.X., et al., 2015. The variation of chemical characteristics of PM_{2.5} and PM₁₀ and formation causes during two haze pollution events in urban Beijing, China. *Atmos. Environ.* 107, 1–8.
- Gu, J.X., Bai, Z.P., Li, W.F., Wu, L.P., Liu, A.X., Dong, H.Y., et al., 2011. Chemical composition of PM_{2.5} during winter in Tianjin, China. *Particology* 9 (3), 215–221.
- Gu, J.X., Bai, Z.P., Liu, A.X., Wu, L.P., Xie, Y.Y., Li, W.F., et al., 2010. Characterization of atmospheric organic carbon and element carbon of PM_{2.5} and PM₁₀ at Tianjin, China. *Aerosol Air Qual. Res.* 10, 167–176.
- Han, S.Q., Wu, J.H., Zhang, Y.F., Cai, Z.Y., Feng, Y.C., Yao, Q., et al., 2014. Characteristics and formation mechanism of a winter haze-fog episode in Tianjin, China. *Atmos. Environ.* 98, 323–330.
- He, H., Wang, Y.S., Ma, Q.X., Ma, J.Z., Chu, B.W., Ji, D.S., et al., 2014. Mineral dust and NO_x promote the conversion of SO₂ to sulfate in heavy pollution days. *Sci. Rep.* 4, 4172.
- He, K.B., Yang, F.M., Ma, Y.L., Zhang, Q., Yao, X.H., Chan, C.C., et al., 2001. The characteristics of PM_{2.5} in Beijing, China. *Atmos. Environ.* 35 (29), 4959–4970.
- Hennigan, C.J., Bergin, M.H., Dibb, J.E., Weber, R.J., 2008. Enhanced secondary organic aerosol formation due to water uptake by fine particles. *Geophys. Res. Lett.* 35 (18), L18801.
- Hu, W.W., Hu, M., Deng, Z.Q., Xiao, R., Kondo, Y., Takegawa, N., et al., 2012. The characteristics and origins of carbonaceous aerosol at a rural site of PRD in summer of 2006. *Atmos. Chem. Phys.* 12 (4), 1811–1822.

- Huang, X.J., Liu, Z.R., Liu, J.Y., Hu, B., Wen, T.X., Tang, G.Q., et al., 2017. Chemical characterization and source identification of PM_{2.5} at multiple sites in the Beijing-Tianjin-Hebei region, China. *Atmos. Chem. Phys.* 17, 12941–12962.
- Ji, D.S., Gao, M., Maenhaut, W., He, J., Wu, C., Cheng, L.J., et al., 2019. The carbonaceous aerosol levels still remain a challenge in the Beijing-Tianjin-Hebei region of China: Insights from continuous high temporal resolution measurements in multiple cities. *Environ. Int.* 126, 171–183.
- Ji, D.S., Li, L., Wang, Y.S., Zhang, J.K., Cheng, M.T., Sun, Y., et al., 2014. The heaviest particulate air-pollution episodes occurred in northern China in January, 2013: Insights gained from observation. *Atmos. Environ.* 92, 546–556.
- Khoder, M.I., 2002. Atmospheric conversion of sulfur dioxide to particulate sulfate and nitrogen dioxide to particulate nitrate and gaseous nitric acid in an urban area. *Chemosphere* 49, 675–684.
- Kong, L.D., Du, C.T., Zhanzakova, A., Cheng, T.T., Yang, X., Wang, L., et al., 2018. Trends in heterogeneous aqueous reaction in continuous haze episodes in suburban Shanghai: An in-depth case study. *Sci. Total Environ.* 634, 1192–1204.
- Li, H.Y., Zhang, Q., Zheng, B., Chen, C.R., Wu, N.N., Guo, H.Y., et al., 2018. Nitrate-driven urban haze pollution during summertime over the North China Plain. *Atmos. Chem. Phys.* 18 (8), 5293–5306.
- Li, R., Cui, L.L., Li, J.L., Zhao, A., Fu, H.B., Wu, Y., et al., 2017. Spatial and temporal variation of particulate matter and gaseous pollutants in China during 2014–2016. *Atmos. Environ.* 161, 235–246.
- Li, W.F., Bai, Z.P., Liu, A. X., Chen, J., Chen, 2009. Characteristics of major PM_{2.5} components during winter in Tianjin, China. *Aerosol Air Qual. Res.* 9 (1), 105–119.
- Lin, P., Hu, M., Deng, Z., Slanina, J., Han, S., Kondo, Y., et al., 2009. Seasonal and diurnal variations of organic carbon in PM_{2.5} in Beijing and the estimation of secondary organic carbon. *J. Geophys. Res.-Atmos.* 114 (D2), D00G11.
- Liu, J., Wu, D., Fan, S.J., Mao, X., Chen, H.Z., 2017a. A one-year, on-line, multi-site observational study on water-soluble inorganic ions in PM_{2.5} over the Pearl River Delta region, China. *Sci. Total Environ.* 601, 1720–1732.
- Liu, T.T., Gong, S.L., He, J.J., Yu, M., Wang, Q.F., Li, H.R., et al., 2017b. Attributions of meteorological and emission factors to the 2015 winter severe haze pollution episodes in China's Jing-Jin-Ji area. *Atmos. Chem. Phys.* 17 (4), 2971–2980.
- Liu, H.J., Liu, X.Y., Wu, Y.M., Liu, W., Bai, X.X., Wang, Y., et al., 2019. Seasonal variation, formation mechanisms and potential sources of PM_{2.5} in two typical cities in the Central Plains Urban Agglomeration, China. *Sci. Total Environ.* 657, 657–670.
- Lu, F., Xu, D.Q., Cheng, Y.B., Dong, S.X., Guo, C., Jiang, X., et al., 2015. Systematic review and meta-analysis of the adverse health effects of ambient PM_{2.5} and PM₁₀ pollution in the Chinese population. *Environ. Res.* 136, 196–204.
- Ma, J.Z., Chu, B.W., Liu, J., Liu, Y.C., Zhang, H.X., He, H., 2018. NO_x promotion of SO₂ conversion to sulfate: An important mechanism for the occurrence of heavy haze during winter in Beijing. *Environ. Pol.* 233, 662–669.
- Ma, Q.X., Wu, Y.F., Zhang, D.Z., Wang, X.J., Xia, Y.J., Liu, X.Y., et al., 2017. Roles of regional transport and heterogeneous reactions in the PM_{2.5} increase during winter haze episodes in Beijing. *Sci. Total Environ.* 599, 246–253.
- Morales, J.A., Pirela, D., de Nava, M.G., de Borrego, B.S., Velásquez, H., Durána, J., 1998. Inorganic water soluble ions in atmospheric particles over Maracaibo Lake Basin in the western region of Venezuela. *Atmos. Res.* 46 (3–4), 0–320.
- Pathak, R.K., Wu, W.S., Wang, T., 2009. Summertime PM_{2.5} ionic species in four major cities of China: nitrate formation in an ammonia-deficient atmosphere. *Atmos. Chem. Phys.* 9, 1711–1722.
- Qiu, X.H., Duan, L., Gao, J., Wang, S.L., Chai, F.H., Hu, J., et al., 2016. Chemical composition and source apportionment of PM₁₀ and PM_{2.5} in different functional areas of Lanzhou, China. *J. Environ. Sci.* 40, 75–83.
- Quan, J.N., Liu, Q., Li, X., Gao, Y., Jia, X.C., Sheng, J.J., et al., 2015. Effect of heterogeneous aqueous reactions on the secondary formation of inorganic aerosols during haze events. *Atmos. Environ.* 122, 306–312.
- Seinfeld, J.H., Pandis, S.N., 2006. *Atmospheric Chemistry and Physics: from Air Pollution to Climate Change* (2nd ed.). John Wiley & Sons, New York.
- Shao, P.Y., Tian, H.Z., Sun, Y.J., Liu, H.J., Wu, B.B., Liu, S.H., et al., 2018. Characterizing remarkable changes of severe haze events and chemical compositions in multi-size airborne particles (PM₁, PM_{2.5} and PM₁₀) from January 2013 to 2016–2017 winter in Beijing, China. *Atmos. Environ.* 189, 133–144.
- Song, Y., Tang, X.Y., Xie, S.D., Zhang, Y.H., Wei, Y.J., Zhang, M.S., et al., 2007. Source apportionment of PM_{2.5} in Beijing in 2004. *J. Hazard. Mater.* 146, 124–130.
- Tai, A.P., Mickle, L.J., Jacob, D.J., 2010. Correlations between fine particulate matter (PM_{2.5}) and meteorological variables in the United States: Implications for the sensitivity of PM_{2.5} to climate change. *Atmos. Environ.* 44 (32), 3976–3984.
- Tian, M., Wang, H.B., Chen, Y., Yang, F.M., Zhang, X.H., Zou, Q., et al., 2016. Characteristics of aerosol pollution during heavy haze events in Suzhou, China. *Atmos. Chem. Phys.* 16 (11), 7357–7371.
- Tian, S.L., Pan, Y.P., Liu, Z., Wen, T.X., Wang, Y.S., 2014. Size-resolved aerosol chemical analysis of extreme haze pollution events during early 2013 in urban Beijing, China. *J. Hazard. Mater.* 279, 452–460.
- Turpin, B.J., Lim, H.J., 2001. Species contributions to PM_{2.5} mass concentrations: Revisiting common assumptions for estimating organic mass. *Aerosol Sci. Technol.* 35, 602–610.
- Wang, G.H., Zhang, R.Y., Gomez, M.E., Yang, L.X., Zamora, M.L., Hu, M., et al., 2016. Persistent sulfate formation from London Fog to Chinese haze. *Proc. Natl. Acad. Sci. USA* 113 (38), 13630–13635.
- Wang, L.T., Wei, Z., Yang, J., Zhang, Y., Zhang, F.F., Su, J., et al., 2014. The 2013 severe haze over northern Hebei, China: Model evaluation, source apportionment, and policy implications. *Atmos. Chem. Phys.* 14, 3151–3173.
- Wang, Q.Z., Zhuang, G.S., Huang, K., Liu, T.N., Deng, C.C., Xu, J., et al., 2015a. Probing the severe haze pollution in three typical regions of China: Characteristics, sources and regional impacts. *Atmos. Environ.* 120, 76–88.
- Wang, L.L., Liu, Z.R., Sun, Y., Ji, D.S., Wang, Y.S., 2015b. Long-range transport and regional sources of PM_{2.5} in Beijing based on long-term observations from 2005 to 2010. *Atmos. Res.* 157, 37–48.
- Wang, P., Cao, J.J., Shen, Z.X., Han, Y.M., Lee, S.C., Huang, Y., et al., 2015c. Spatial and seasonal variations of PM_{2.5} mass and species during 2010 in Xi'an, China. *Sci. Total Environ.* 508, 477–487.
- Wang, X.Q., Wei, W., Cheng, S.Y., Li, J.B., Zhang, H.Y., Lv, Z., 2018. Characteristics and classification of PM_{2.5} pollution episodes in Beijing from 2013 to 2015. *Sci. Total Environ.* 612, 170–179.
- Watson, J.G., Chow, J.C., Houck, J.E., 2001. PM_{2.5} chemical source profiles for vehicle exhaust, vegetative burning, geological material, and coal burning in Northwestern Colorado during 1995. *Chemosphere* 43, 1141–1151.
- Xu, H., Xiao, Z.M., Chen, K., Tang, M., Zheng, N.Y., Li, P., et al., 2019. Spatial and temporal distribution, chemical characteristics, and sources of ambient particulate matter in the Beijing-Tianjin-Hebei region. *Sci. Total Environ.* 658, 280–293.
- Xu, L.H., Batterman, S., Chen, F., Li, J.B., Zhong, X.F., Feng, Y.J., et al., 2017. Spatiotemporal characteristics of PM_{2.5} and PM₁₀ at urban and corresponding background sites in 23 cities in China. *Sci. Total Environ.* 599–600, 2074–2084.
- Xue, J., Yuan, Z.B., Griffith, S.M., Yu, X., Lau, A.K.H., Yu, J.Z., 2016. Sulfate formation enhanced by a cocktail of high NO_x, SO₂, particulate matter, and droplet pH during haze-fog events in megacities in China: An observation-based modeling investigation. *Environ. Sci. Technol.* 50 (14), 7325–7334.
- Yang, L.X., Gao, X.M., Wang, X.F., Nie, W., Wang, J., Gao, R., et al., 2014. Impacts of firecracker burning on aerosol chemical characteristics and human health risk levels during the Chinese New Year Celebration in Jinan, China. *Sci. Total Environ.* 476–477, 57–64.
- Yang, S., Ma, Y.L., Duan, F.K., He, K.B., Wang, L.T., Wei, Z., et al., 2018. Characteristics and formation of typical winter haze in Handan, one of the most polluted cities in China. *Sci. Total Environ.* 613–614, 1367–1375.
- Yang, Y.R., Liu, X.G., Qu, Y., Wang, J.L., An, J.L., Zhang, Y.H., 2015. Formation mechanism of continuous extreme haze episodes in the megacity Beijing, China, in January 2013. *Atmos. Res.* 155, 192–203.
- Yuan, J., Liu, B.S., Cheng, Y., Xiao, Z.M., Xu, H., Guan, Y.C., 2018. Study on characteristics of PM_{2.5} and chemical components and source apportionment of high temporal resolution in January 2017 in Tianjin urban area. *Acta Scientiae Circumstantiae* 38 (3), 1090–1101.
- Zhang, Q., Shen, Z.X., Cao, J.J., Zhang, R.J., Zhang, L.M., Huang, R.J., et al., 2015. Variations in PM_{2.5}, TSP, BC, and trace gases (NO₂, SO₂, and O₃) between haze and non-haze episodes in winter over Xi'an, China. *Atmos. Environ.* 112, 64–71.
- Zhao, P.S., Dong, F., He, D., Zhao, X.J., Zhang, X.L., Zhang, W.Z., et al., 2013a. Characteristics of concentrations and chemical compositions for PM_{2.5} in the region of Beijing, Tianjin, and Hebei, China. *Atmos. Chem. Phys.* 13 (9), 4631–4644.
- Zhao, P.S., Dong, F., Yang, Y.D., He, D., Zhao, X.J., Zhang, W.Z., et al., 2013b. Characteristics of carbonaceous aerosol in the region of Beijing, Tianjin, and Hebei, China. *Atmos. Environ.* 71, 389–398.
- Zheng, G.J., Duan, F.K., Su, H., Ma, Y.L., Cheng, Y., Zheng, B., et al., 2015. Exploring the severe winter haze in Beijing: the impact of synoptic weather, regional transport and heterogeneous reactions. *Atmos. Chem. Phys.* 15 (6), 2969–2983.